

# Electrical Characteristics of Microelectronic GaN based HEMTs at the AlGa<sub>N</sub> Thickness of 10 nm

*Subhadeep Mukhopadhyay\**

Department of Electronics and Communication Engineering, National Institute of Technology  
Arunachal Pradesh, Yupia, Papum Pare, Arunachal Pradesh, India

## Abstract

*In this work, total 3655 individual simulation-outputs are reported. Total 25 individual microelectronic single-heterojunction AlGa<sub>N</sub>/GaN high electron mobility transistor (HEMT) structures are designed and simulated in this work using the SILVACO-ATLAS software tool. In this work, drain voltage and gate voltage are electrical parameters. Aluminium mole fraction and gate length are structural parameters. The effect of drain voltage on drain current is studied. The effect of gate voltage on drain current is studied. Also, the effect of aluminium mole fraction on drain current is studied. As an effect, the drain current reduces due to larger gate length. This work will be helpful to experimentally fabricate the microelectronic HEMT structures.*

**Keywords:** Mole fraction, Drain current, Drain voltage, Gate voltage, Gate length

\***Author for Correspondence** E-mail: subhadeepmukhopadhyay21@gmail.com

## INTRODUCTION

Recently, Mukhopadhyay as author has investigated the electrical characteristics of GaN based single-heterojunction and double-heterojunction HEMTs from the aspects of microelectronics and Nanoelectronics [1–3]. Charfeddine et al. have studied the device characteristics of GaN based single-heterojunction HEMTs on the basis of analytical modeling along with the consideration of Kink effect [4]. Chattopadhyay et al. have developed the analytical models to study the device characteristics of GaN based HEMTs [5–8].

Khandelwal et al. have developed an analytical model to analyze the 2DEG charge density in AlGa<sub>N</sub>/GaN HEMT devices [9]. Also, Khandelwal et al. have developed another analytical Model to analyze the surface-potential and intrinsic charges in AlGa<sub>N</sub>/GaN HEMT devices [10]. Khandelwal et al. have proposed a robust surface-potential-based compact model for GaN HEMT IC design [11]. They have proposed the physics based compact model of I-V and C-V characteristics related to the AlGa<sub>N</sub>/GaN HEMT devices [12].

In the present work, author has studied the dependence of drain current on drain voltage

and gate voltage in microelectronic single-heterojunction AlGa<sub>N</sub>/GaN HEMT devices. Also, author has studied the dependence of drain current on aluminium mole fraction. Finally, author has studied the effect of gate length on drain current. This work will be helpful to experimentally fabricate the microelectronic AlGa<sub>N</sub>/GaN HEMTs.

## DESIGNS OF DEVICES

In this work, a representative cross-sectional view of the microelectronic single-heterojunction AlGa<sub>N</sub>/GaN HEMT structures is shown in Figure 1. The cross-sectional dimensions of different portions of these designed HEMT-structures are given below: (A) Source dimensions are 500 nm (length)×100 nm (height); (B) Drain dimensions are 500 nm (length)×100 nm (height); (C) Gate dimensions are  $L_G$  (length)×500 nm (height); (D) Total horizontal length of the device is 9500 nm; (E) GaN thickness is 500 nm; (F) Sapphire thickness is 1000 nm; and (G) Source to gate fixed distance is 3000 nm. In this work, the gate length ( $L_G$ ) is varied with the following lengths as 1.5, 2.0, 2.5, 3.0, and 3.5 micron. With the variation in gate length, the source to gate distance is fixed (3000 nm), but the gate to drain distance is variable. The selected

thickness of AlGaN nano-layer is 10 nm. The selected aluminium mole fractions ( $x$ ) are 0.10, 0.15, 0.20, 0.25, and 0.30. Therefore, total 25 individual HEMT-structures are designed and simulated. GaN and sapphire are chosen as the materials to design the HEMT structures according to the already reported comparative material properties with respect to other materials [1, 2]. In this work, the AlGaN doping concentration is maintained as  $1 \times 10^{18} \text{ cm}^{-3}$  in each HEMT structure.

## RESULTS AND DISCUSSION

### Effects of Drain Voltage and Gate Voltage on Drain Current

From the Figures 2 to 6, the effects of drain voltage ( $V_D$ ) and gate voltage ( $V_G$ ) on drain current are shown corresponding to the gate length ( $L_G$ ) of 1.5 micron. According to the Figure 2, the drain current increases with drain voltage at any particular aluminium mole fraction ( $x$ ) corresponding to the gate voltage ( $V_G$ ) of 0 Volt [1–3]. According to the Figure 3, the drain current increases with drain voltage at any particular aluminium mole fraction ( $x$ ) corresponding to the gate voltage ( $V_G$ ) of -1 Volt [1–3]. According to the Figure 4, the drain current increases with drain voltage at any particular aluminium mole fraction ( $x$ ) corresponding to the gate voltage ( $V_G$ ) of -2 Volts [1–3]. In the Figure 5, the drain current increases with drain voltage at

the aluminium mole fraction ( $x$ ) of 0.30, but no significant change is observed at the aluminium mole fractions ( $x$ ) of 0.10, 0.15, 0.20 and 0.25 corresponding to the gate voltage ( $V_G$ ) of -3 Volt [1–3]. In the Figure 6, the drain current increases with increasing gate voltage at any particular aluminium mole fraction ( $x$ ) corresponding to the drain voltage ( $V_D$ ) of 1 Volt [1–3].

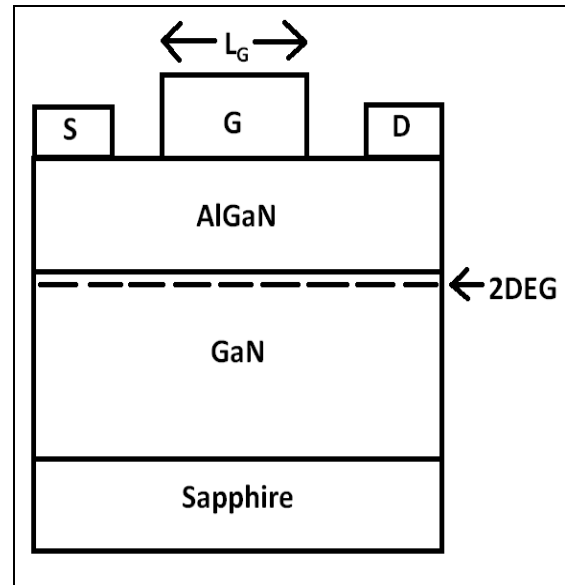


**Fig. 1:** Representative Schematic Diagram of Microelectronic Single-heterojunction AlGaN/GaN High Electron Mobility Transistor is shown.

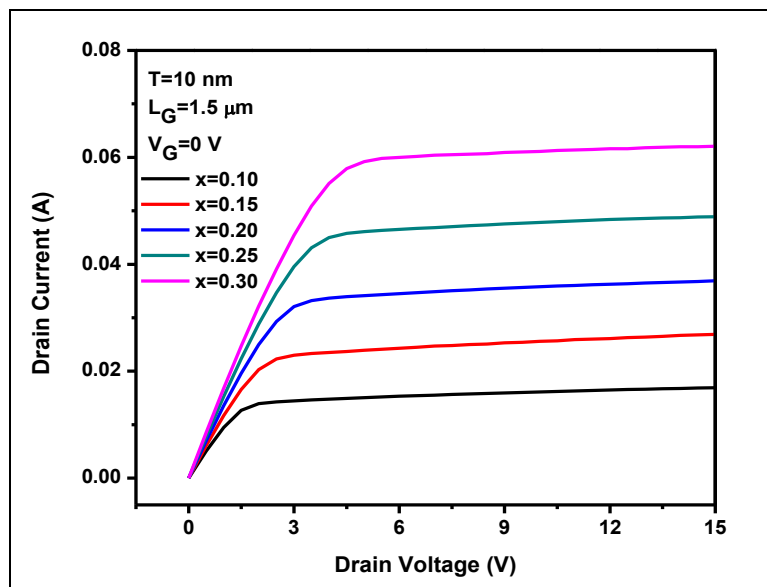


**Fig. 2:** The Variation of Drain Current with Respect to Drain Voltage is shown Corresponding to the Gate Voltage ( $V_G$ ) of 0 volt, Gate Length ( $L_G$ ) of 1.5 micron and AlGaN Thickness ( $T$ ) of 10 nm. The Variation of Drain Current is also shown with Respect to Aluminium Mole Fraction ( $x$ ).

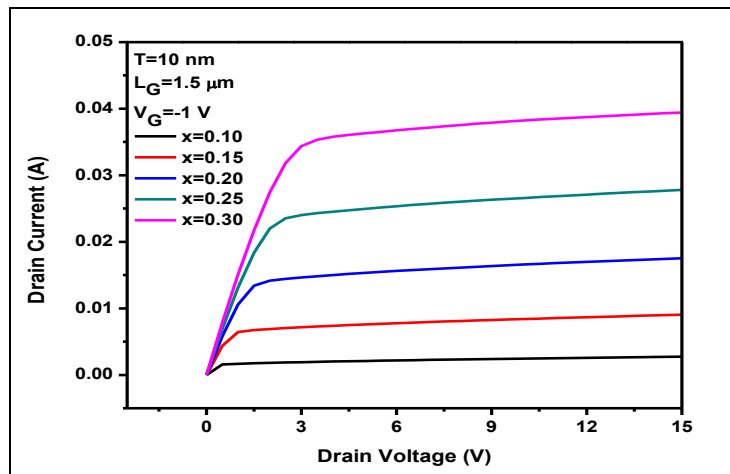


**Fig. 3:** The Variation of Drain Current with Respect to Drain Voltage is shown Corresponding to the Gate Voltage ( $V_G$ ) of -1 volt, Gate Length ( $L_G$ ) of 1.5 micron and AlGaIn Thickness ( $T$ ) of 10 nm. The Variation of Drain Current is also shown with Respect to Aluminium Mole Fraction ( $x$ ).

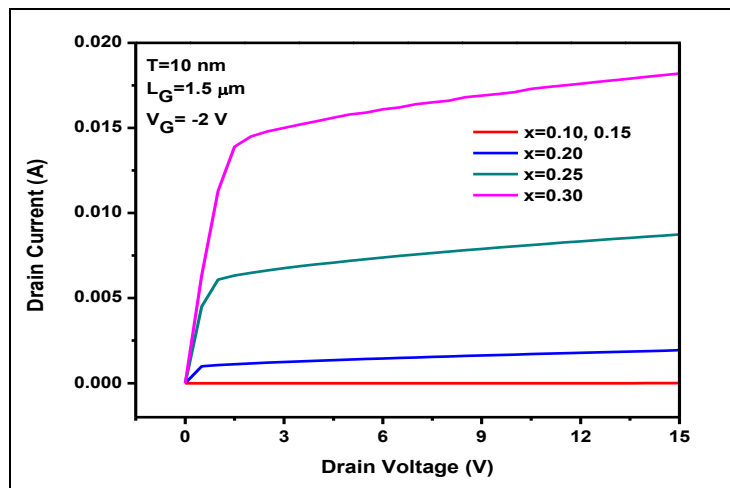


**Fig. 4:** The Variation of Drain Current with Respect to Drain Voltage is shown Corresponding to the Gate Voltage ( $V_G$ ) of -2 volt, Gate Length ( $L_G$ ) of 1.5 micron and AlGaIn Thickness ( $T$ ) of 10 nm. The Variation of Drain Current is also shown with Respect to Aluminium Mole Fraction ( $x$ ).

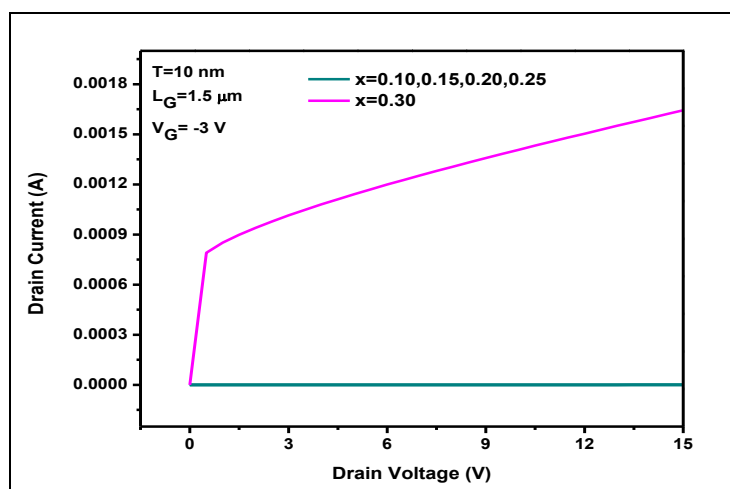


**Fig. 5:** The Variation of Drain Current with Respect to Drain Voltage is shown Corresponding to the Gate Voltage ( $V_G$ ) of -3 volt, Gate Length ( $L_G$ ) of 1.5 micron and AlGaIn Thickness ( $T$ ) of 10 nm. The Variation of Drain Current is also shown with Respect to Aluminium Mole Fraction ( $x$ ).

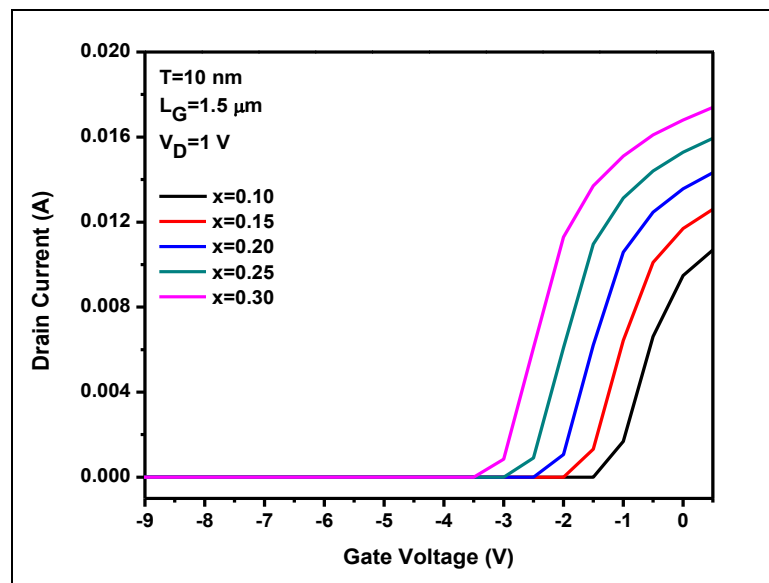


**Fig. 6:** The Variation of Drain Current with Respect to Gate Voltage is shown Corresponding to the Drain Voltage ( $V_D$ ) of 1 volt, Gate Length ( $L_G$ ) of 1.5 micron and AlGaIn Thickness ( $T$ ) of 10 nm. The Variation of Drain Current is also shown with Respect to Aluminium Mole Fraction ( $x$ ).

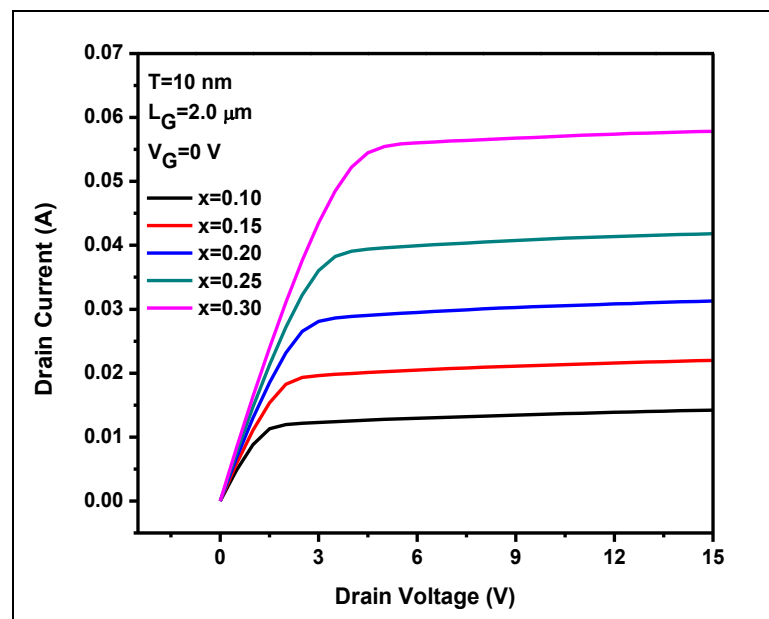


**Fig. 7:** The Variation of Drain Current with Respect to Drain Voltage is shown Corresponding to the Gate Voltage ( $V_G$ ) of 0 volt, Gate Length ( $L_G$ ) of 2.0 micron and AlGaIn Thickness ( $T$ ) of 10 nm. The Variation of Drain Current is also shown with Respect to Aluminium Mole Fraction ( $x$ ).

From the Figures 7 to 10, the effects of drain voltage ( $V_D$ ) and gate voltage ( $V_G$ ) on drain current are shown corresponding to the gate length ( $L_G$ ) of 2.0 micron. In the Figure 7, the drain current increases with increasing drain voltage at any particular aluminium mole fraction ( $x$ ) corresponding to the gate voltage ( $V_G$ ) of 0 Volt [1–3]. According to the Figure 8, the drain current increases with increasing drain voltage at any particular aluminium mole

fraction ( $x$ ) corresponding to the gate voltage ( $V_G$ ) of -1 Volt [1–3]. Similar trends in variation of drain current are observed in Figure 9 corresponding to the gate voltage ( $V_G$ ) of -2 Volts [1–3]. In the Figure 10, the drain current increases with drain voltage at the aluminium mole fraction ( $x$ ) of 0.30, but no significant increase is observed at the mole fractions ( $x$ ) of 0.10, 0.15, 0.20 and 0.25 corresponding to the gate voltage ( $V_G$ ) of -3 Volts [1–3].

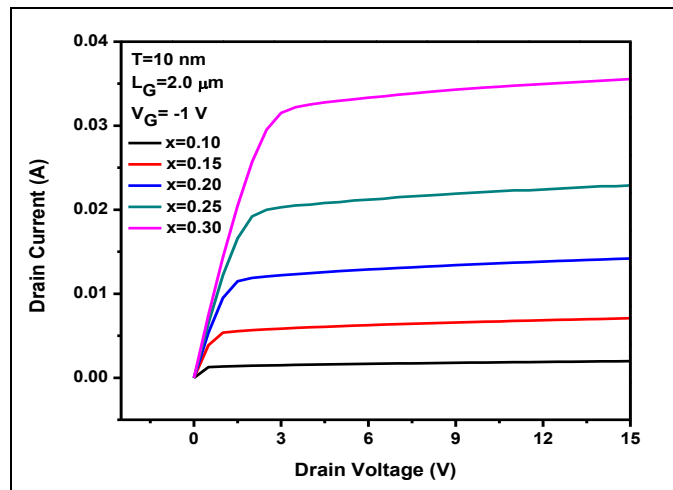


**Fig. 8:** The Variation of Drain Current with Respect to Drain Voltage is shown Corresponding to the Gate Voltage ( $V_G$ ) of -1 volt, Gate Length ( $L_G$ ) of 2.0 micron and AlGaIn Thickness ( $T$ ) of 10 nm. The Variation of Drain Current is also shown with Respect to Aluminium Mole Fraction ( $x$ ).

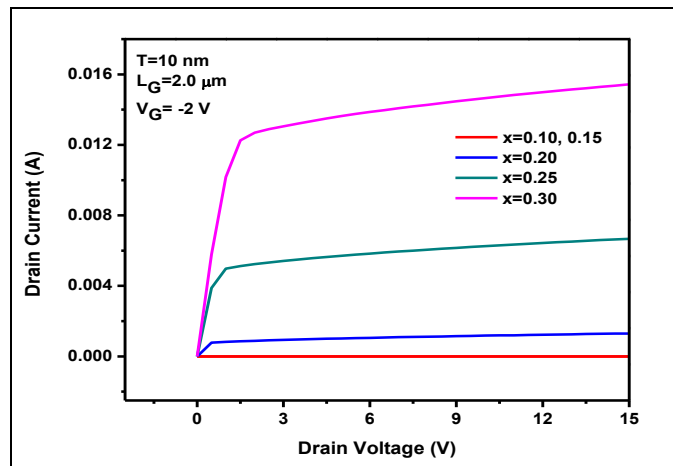


**Fig. 9:** The Variation of Drain Current with Respect to Drain Voltage is Shown Corresponding to the Gate Voltage ( $V_G$ ) of -2 volt, Gate Length ( $L_G$ ) of 2.0 micron and AlGaIn Thickness ( $T$ ) of 10 nm. The Variation of Drain Current is also shown with Respect to Aluminium Mole Fraction ( $x$ ).

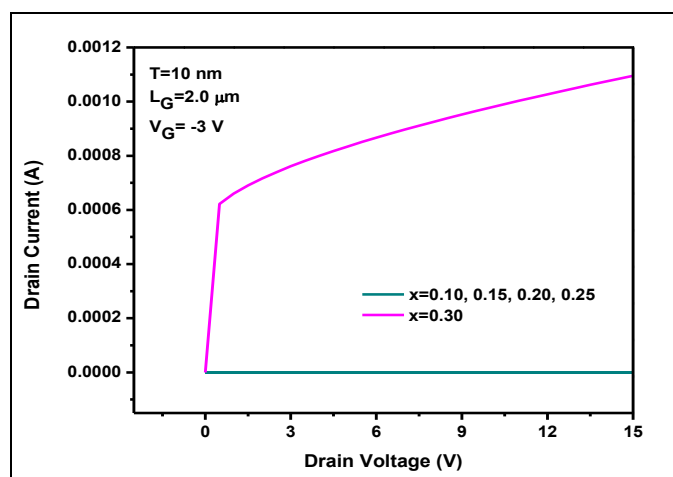


**Fig. 10:** The Variation of Drain Current with Respect to Drain Voltage is shown Corresponding to the Gate Voltage ( $V_G$ ) of -3 volt, Gate Length ( $L_G$ ) of 2.0 micron and AlGaIn Thickness ( $T$ ) of 10 nm. The Variation of Drain Current is also shown with Respect to Aluminium Mole Fraction ( $x$ ).

From the Figures 11 to 14, similar trends in dependence of drain current on drain voltage and gate voltage are observed corresponding to the gate length ( $L_G$ ) of 2.5 micron [1–3]. Figures 15 to 18 show similar trends in

dependence of drain current corresponding to the gate length ( $L_G$ ) of 3.0 micron [1–3]. Also, Figures 19 to 23 show similar trends in dependence of drain current corresponding to the gate length ( $L_G$ ) of 3.5 micron [1–3].

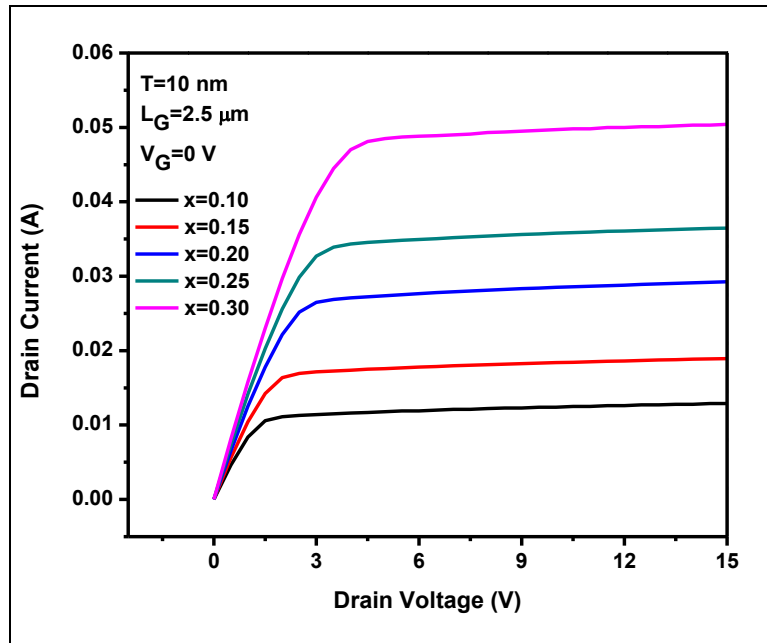


**Fig. 11:** The Variation of Drain Current with Respect to Drain Voltage is shown Corresponding to the Gate Voltage ( $V_G$ ) of 0 volt, Gate Length ( $L_G$ ) of 2.5 micron and AlGaN Thickness ( $T$ ) of 10 nm. The Variation of Drain Current is also shown with Respect to Aluminium Mole Fraction ( $x$ ).

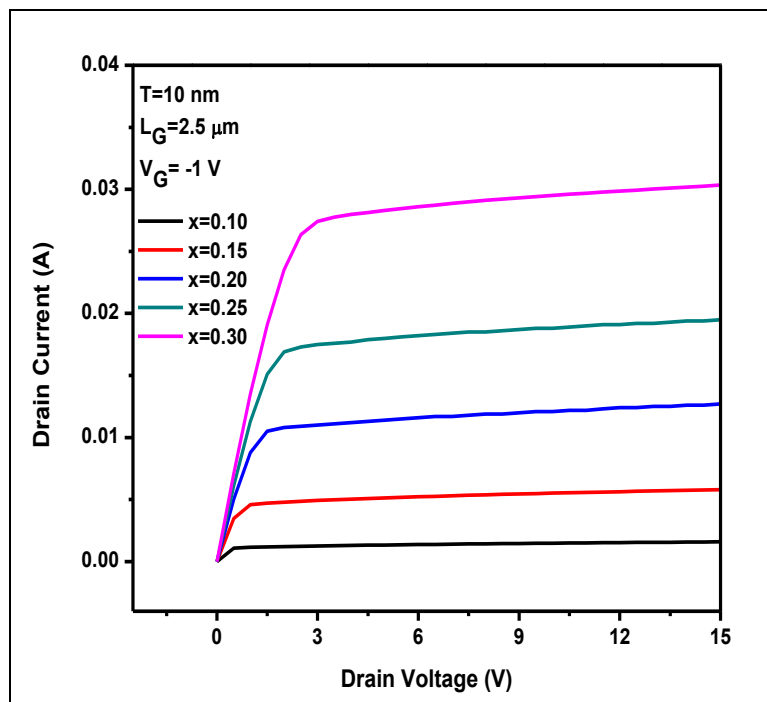


**Fig. 12:** The Variation of Drain Current with Respect to Drain Voltage is shown Corresponding to the Gate Voltage ( $V_G$ ) of -1 volt, Gate Length ( $L_G$ ) of 2.5 micron and AlGaN Thickness ( $T$ ) of 10 nm. The Variation of Drain Current is also shown with Respect to Aluminium Mole Fraction ( $x$ ).

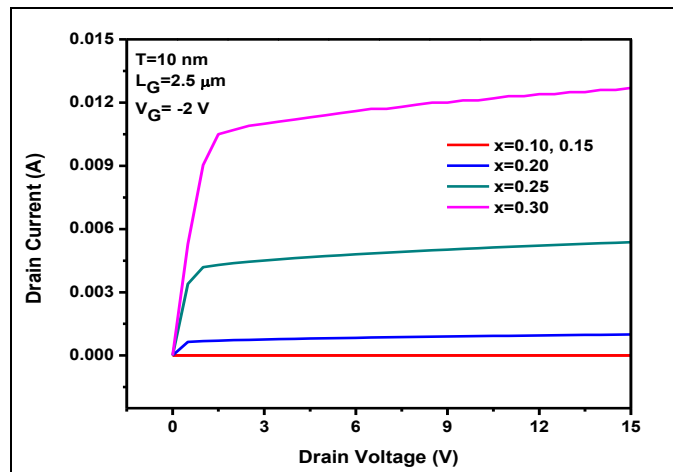


**Fig. 13:** The Variation of Drain Current with Respect to Drain Voltage is shown Corresponding to the Gate Voltage ( $V_G$ ) of -2 volt, Gate Length ( $L_G$ ) of 2.5 Micron and AlGa<sub>N</sub> Thickness ( $T$ ) of 10 nm. The Variation of Drain Current is also shown with Respect to Aluminium Mole Fraction ( $x$ ).

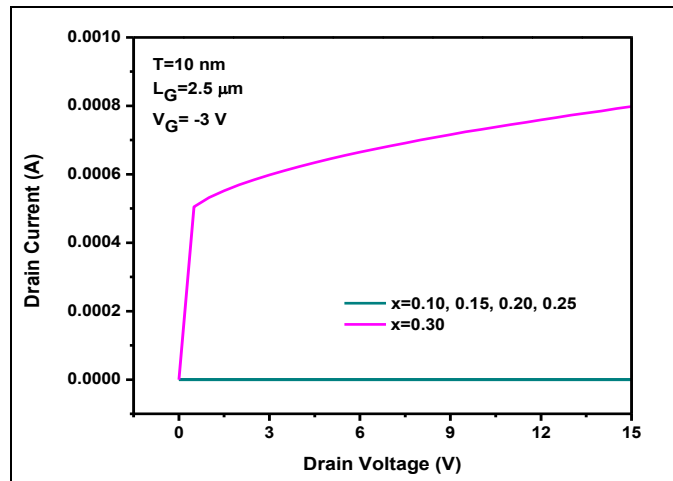


**Fig. 14:** The Variation of Drain Current with Respect to Drain Voltage is shown Corresponding to the Gate Voltage ( $V_G$ ) of -3 volt, Gate Length ( $L_G$ ) of 2.5 micron and AlGa<sub>N</sub> Thickness ( $T$ ) of 10 nm. The Variation of Drain Current is also shown with Respect to Aluminium Mole Fraction ( $x$ ).

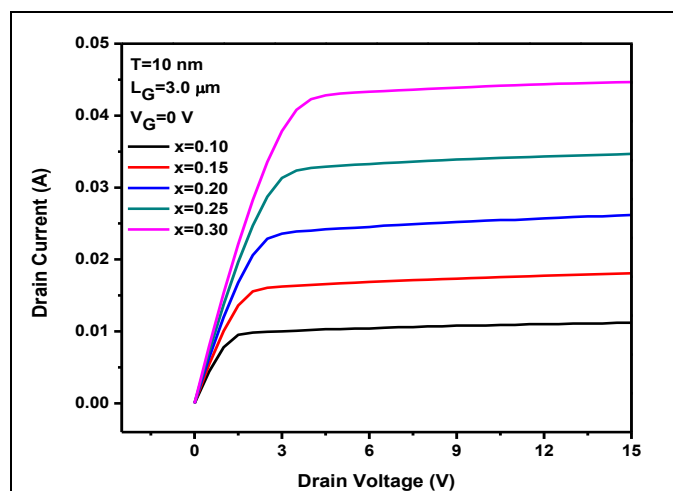


**Fig. 15:** The Variation of Drain Current with Respect to Drain Voltage is shown Corresponding to the Gate Voltage ( $V_G$ ) of 0 volt, Gate Length ( $L_G$ ) of 3.0 micron and AlGa<sub>N</sub> Thickness ( $T$ ) of 10 nm. The Variation of Drain Current is also shown with Respect to Aluminium Mole Fraction ( $x$ ).

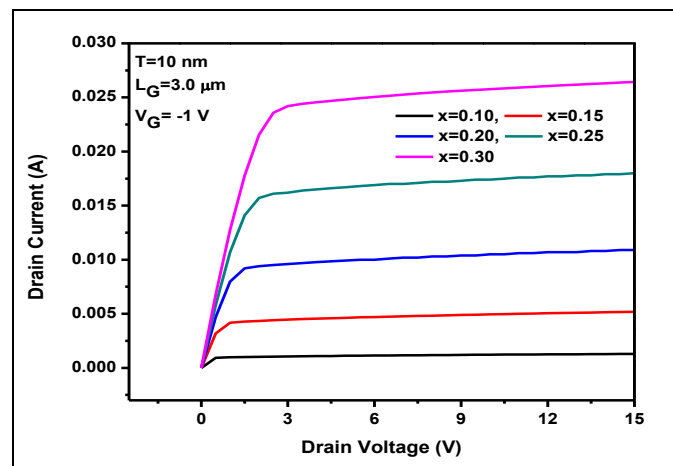


**Fig. 16:** The Variation of Drain Current with Respect to Drain Voltage is shown Corresponding to the Gate Voltage ( $V_G$ ) of -1 volt, Gate Length ( $L_G$ ) of 3.0 micron and AlGaIn Thickness ( $T$ ) of 10 nm. The Variation of Drain Current is also shown with Respect to Aluminium Mole Fraction ( $x$ ).

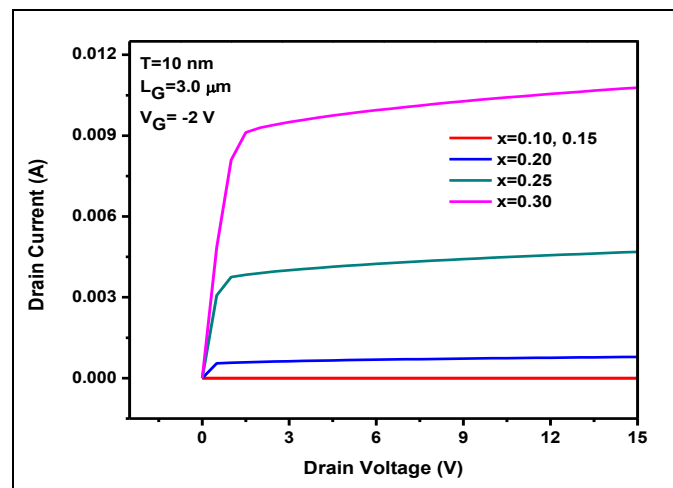


**Fig. 17:** The Variation of Drain Current with Respect to Drain Voltage is shown Corresponding to the Gate Voltage ( $V_G$ ) of -2 volt, Gate Length ( $L_G$ ) of 3.0 micron and AlGaIn Thickness ( $T$ ) of 10 nm. The Variation of Drain Current is also shown with Respect to Aluminium Mole Fraction ( $x$ ).

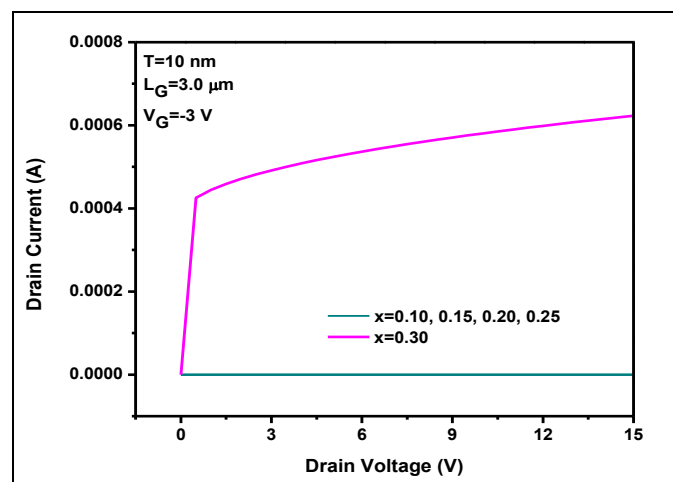


**Fig. 18:** The Variation of Drain Current with Respect to Drain Voltage is shown Corresponding to the Gate Voltage ( $V_G$ ) of -3 volt, Gate Length ( $L_G$ ) of 3.0 micron and AlGaIn Thickness ( $T$ ) of 10 nm. The Variation of Drain Current is also shown with Respect to Aluminium Mole Fraction ( $x$ ).

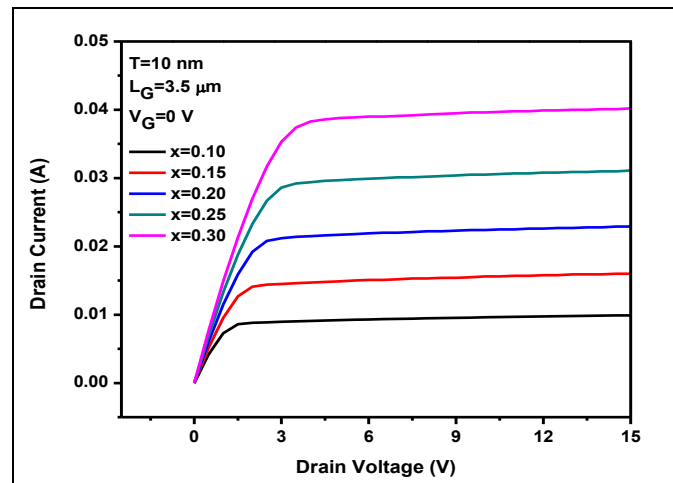


**Fig. 19:** The Variation of Drain Current with Respect to Drain Voltage is shown Corresponding to the Gate Voltage ( $V_G$ ) of 0 volt, Gate Length ( $L_G$ ) of 3.5 micron and AlGaIn Thickness ( $T$ ) of 10 nm. The Variation of Drain Current is also shown with Respect to Aluminium Mole Fraction ( $x$ ).

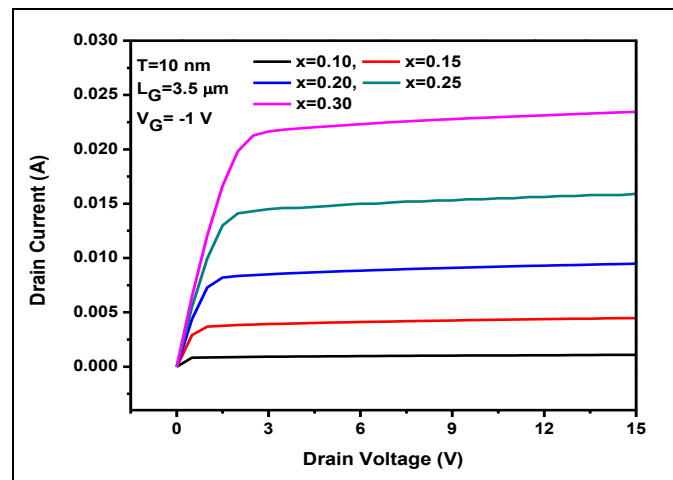


**Fig. 20:** The Variation of Drain Current with Respect to Drain Voltage is shown Corresponding to the Gate Voltage ( $V_G$ ) of -1 volt, Gate Length ( $L_G$ ) of 3.5 micron and AlGaIn Thickness ( $T$ ) of 10 nm. The Variation of Drain Current is also shown with Respect to Aluminium Mole Fraction ( $x$ ).

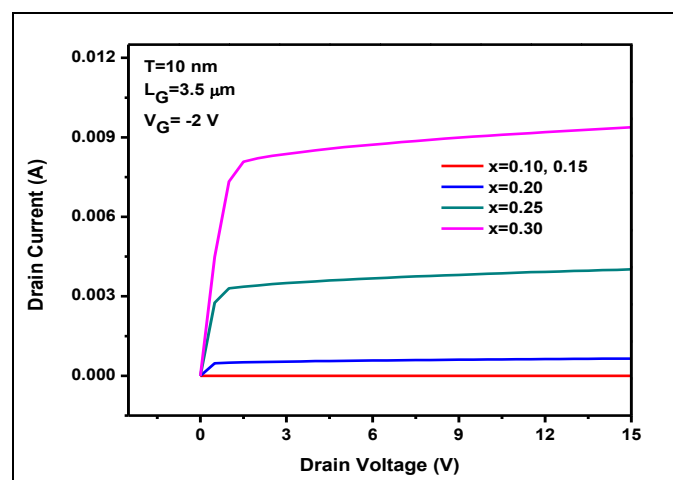


**Fig. 21:** The Variation of Drain Current with Respect to Drain Voltage is shown Corresponding to the Gate Voltage ( $V_G$ ) of -2 volt, Gate Length ( $L_G$ ) of 3.5 micron and AlGaIn Thickness ( $T$ ) of 10 nm. The Variation of Drain Current is also shown with Respect to Aluminium Mole Fraction ( $x$ ).

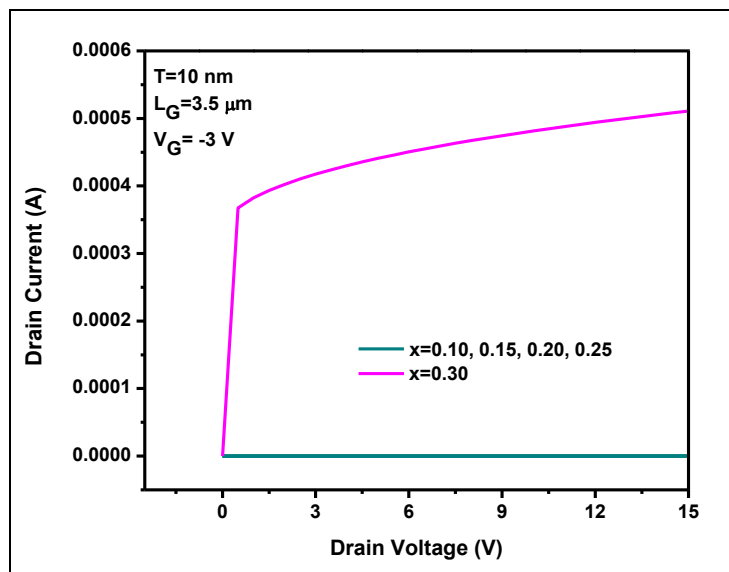


**Fig. 22:** The Variation of Drain Current with Respect to Drain Voltage is shown Corresponding to the Gate Voltage ( $V_G$ ) of -3 volt, Gate Length ( $L_G$ ) of 3.5 micron and AlGaIn Thickness ( $T$ ) of 10 nm. The Variation of Drain Current is also shown with Respect to Aluminium Mole Fraction ( $x$ ).

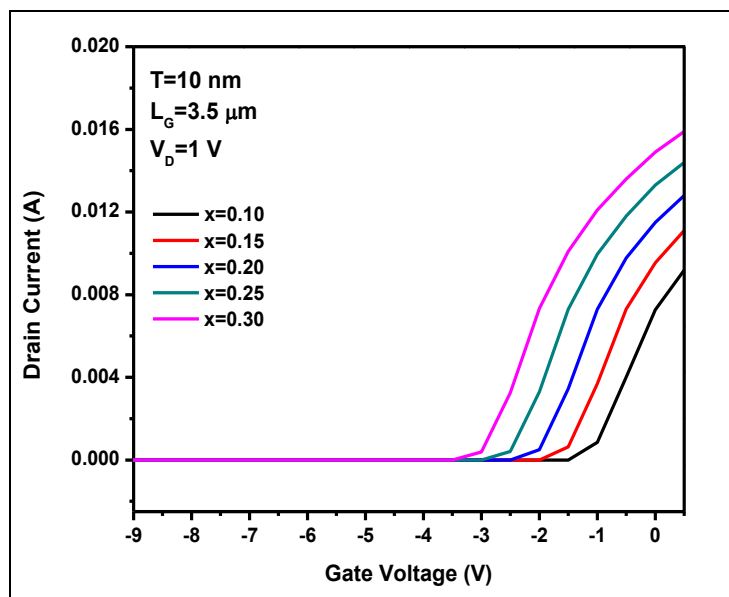


**Fig. 23:** The Variation of Drain Current with Respect to Gate Voltage is shown Corresponding to the Drain Voltage ( $V_D$ ) of 1 volt, Gate Length ( $L_G$ ) of 3.5 micron and AlGaIn Thickness ( $T$ ) of 10 nm. The Variation of Drain Current is also shown with Respect to Aluminium Mole Fraction ( $x$ ).

### Effect of Aluminium Mole Fraction on Drain Current

According to the Figures 2 to 6, the drain current is higher at larger aluminium mole fraction ( $x$ ) corresponding to the gate length ( $L_G$ ) of 1.5 micron [1, 2]. According to the Figures 7 to 10, the drain current is higher at larger aluminium mole fraction ( $x$ ) corresponding to the gate length ( $L_G$ ) of 2.0 micron [1, 2]. Also, according to the Figures 11 to 14, similar trends in dependence of drain

current on mole fraction ( $x$ ) is observed corresponding the gate length ( $L_G$ ) of 2.5 micron [1, 2]. Similarly, according to the Figures 15 to 18, higher drain current is observed at larger mole fraction ( $x$ ) corresponding to the gate length ( $L_G$ ) of 3.0 micron [1, 2]. Again, according to the Figures 19 to 23, higher drain current is observed at larger mole fraction ( $x$ ) corresponding to the gate length of 3.5 micron [1, 2].

### Effect of Gate Length on Drain Current

According to the Figures 2, 7, 11, 15, and 19, the drain current reduces at larger gate length ( $L_G$ ) corresponding to the gate voltage ( $V_G$ ) of 0 Volt [1–3, 4]. According to the Figures 3, 8, 12, 16, and 20, the drain current reduces at larger gate length ( $L_G$ ) corresponding to the gate voltage ( $V_G$ ) of -1 Volt [1–3, 4]. According to the Figures 4, 9, 13, 17, and 21, the drain current reduces at larger gate length ( $L_G$ ) corresponding to the gate voltage ( $V_G$ ) of -2 Volt [1–3, 4]. Also, according to the Figures 5, 10, 14, 18, and 22, the drain current reduces at larger gate length ( $L_G$ ) corresponding to the gate voltage ( $V_G$ ) of -3 Volt [1–3, 4]. Now, the drain current reduces at larger gate length ( $L_G$ ) according to the Figures 6 and 23 [1–3, 4]. Charfeddine et al. have obtained similar effect of gate length on drain current [4].

### CONCLUSIONS

Total 3655 individual simulation-outputs are reported in this work. Total 25 individual microelectronic HEMT structures are designed and simulated in this work using the SILVACO-ATLAS software tool. The drain current increases with increasing drain voltage. The drain current increases with increasing gate voltage. The drain current increases at higher aluminium mole fraction in AlGa<sub>n</sub>N nano-layer. The drain current reduces due to larger gate length. This work will be helpful to fabricate the microelectronic HEMT structures experimentally.

### REFERENCES

1. Mukhopadhyay S, Kalita S. Report on the Effects of Mole Fraction, Doping Concentration, Gate Length and Nano-Layer Thickness to Control the Device Engineering in the Nanoelectronic AlGa<sub>n</sub>N/GaN HEMTs at 300 K to Enhance the Reputation of the National Institute of Technology Arunachal Pradesh, *Nano Trends*. 2017; 19: 15–47p.
2. Mukhopadhyay S. Report on the Novel Electrical Characteristics of Microelectronic High Electron Mobility Transistors to Establish a Low-Cost Microelectronics Laboratory in the National Institute of Technology Arunachal Pradesh, *J Semiconductor Devices Circuits*. 2017; 4: 6–28p.
3. Mukhopadhyay S, Kalita S. Novel Effect of Gate Length on the Electrical Characteristics of Nanoelectronic Double-Heterojunction HEMTs with the Circuit Symbols and Load Line to Configure the Common-Source Amplifiers in Analog Electronics, *Research & Reviews: A J Embedded Syst Appl*. 2017; 5: 8–18p.
4. Charfeddine M, Belmabrouk H, Zaidi MA, et al. 2-D Theoretical Model for Current-Voltage Characteristics in AlGa<sub>n</sub>N/GaN HEMTs, *J Modern Phys*. 2012; 3: 881–886p.
5. Chattopadhyay MK, Tokekar S. Thermal model for dc characteristics of AlGa<sub>n</sub>N/GaN HEMTs including self-heating effect and non-linear polarization, *Microelectr J*. 2008; 39: 1181–1188p.
6. Chattopadhyay MK, Tokekar S. Temperature and polarization dependent polynomial based non-linear analytical model for gate capacitance of Al<sub>m</sub>Ga<sub>1-m</sub>N/GaN MODFET, *Solid-State Electron*. 2006; 50: 220–227p.
7. Korwal M, Haldar S, Gupta M, et al. Parasitic Resistance and Polarization-Dependent Polynomial-Based Non-Linear Analytical Charge-Control Model for AlGa<sub>n</sub>N/GaN MODFET for Microwave Frequency Applications, *Microw Opt Tech Lett*. 2003; 38: 371–378p.
8. Chattopadhyay MK, Tokekar S. Analytical Model for the Transconductance of Microwave Al<sub>m</sub>Ga<sub>1-m</sub>N/GaN HEMTs including nonlinear Macroscopic Polarization and Parasitic MESFET conduction, *Microw Opt Tech Lett*. 2007; 49: 382–389p.
9. Khandelwal S, Goyal N, Fjeldly TA. A Physics-based Analytical Model for 2DEG Charge Density in AlGa<sub>n</sub>N/GaN HEMT Devices, *IEEE T Electron Dev*. 2011; 58: 3622–3625p.
10. Khandelwal S, Chauhan YS, Fjeldly TA. Analytical Modeling of Surface-Potential and Intrinsic Charges in AlGa<sub>n</sub>N/GaN HEMT Devices, *IEEE T Electron Dev*. 2012; 59: 2856–2860p.
11. Khandelwal S, Yadav C, Agnihotri S, et al. Robust Surface-Potential-Based Compact Model for GaN HEMT IC Design, *IEEE T Electron Dev*. 2013; 60: 3216–3222p.

12. Khandelwal S, Fjeldly TA. A physics based compact model of I-V and C-V characteristics in AlGa<sub>N</sub>/Ga<sub>N</sub> HEMT Devices, *Solid-State Electron.* 2012; 76: 60–66p.

**Cite this Article**

Subhadeep Mukhopadhyay. Electrical Characteristics of Microelectronic GaN based HEMTs at the AlGa<sub>N</sub> Thickness of 10 nm. *Research & Reviews: Journal of Physics.* 2018; 7(1): 12–23p.